Facile approach to the synthesis of 3D platinum nanoflowers and their electrochemical characteristics

Jitendra N. Tiwari,*[a] Fu-Ming Pan*[a] and Kun-Lin Lin[b]

Received (in Montpellier, France) 25th November 2008, Accepted 30th January 2009
First published as an Advance Article on the web 6th March 2009
DOI: 10.1039/b901534p

Three-dimensional (3D) platinum nanoflowers have been successfully synthesized by potentiostatic pulse plating method on a silicon substrate, and electrochemical study shows that the nanostructured Pt catalyst has an excellent electrocatalytic activity toward methanol and CO oxidation due to preferential (100) and (110) surface orientations on the Pt nanoflowers.

Introduction

Recently, the synthesis of nanostructured materials with a high specific surface area has attracted great interest in the development of fuel cell catalysts,[1] applications for photocatalytic activity,[2] biosensors,[3] chemical sensors,[4] and in the reduction of pollutant emission from automobiles.[5] Among all precious catalyst metals, platinum has unique chemical and physical characteristics and has a wide range of industrial and environmental applications. However, a critical problem with Pt catalysts is the high cost due to limited supply. Thus, one of the major challenges in fuel cell development is to reduce the usage of platinum catalyst. One effective approach to accomplish this goal is to synthesize Pt nanostructures well dispersed on the electrode so that a high surface/volume ratio can be obtained. In this work, we report a new and facile method of synthesizing 3D platinum nanoflowers on a silicon substrate by potentiostatic pulse plating. The 3D nanostructured platinum catalyst shows excellent electrocatalytic activity toward oxidation of methanol and CO adspecies.

Results and discussion

Surface morphology of the 3D Pt nanoflowers was investigated by scanning electron microscopy (SEM). Fig. 1(A) shows an SEM micrograph of the bipolar-pulse electrodeposited Pt catalyst thin film, which was composed of rose-like particles with a size between ~400 and ~800 nm. The X-ray photoelectron spectrum (XPS) of the 3D Pt nanoflowers is shown in Fig. 1(B). Because the nanoflowers did not fully cover the Si substrate, O 1s and Si 2p XPS signals from the native silicon oxide could still be detected. The binding energies of Pt $4f_{7/2}$ and $4f_{5/2}$ electrons were 71.4 and 74.7 eV, respectively, which are in good agreement with pure bulk platinum.[6] No XPS signal associated with oxidized Pt species (such as Pt^{2+} and Pt^{4+}) and chlorine from the Pt precursor were observed, suggesting that metallic platinum was likely the only constituent of the nanoflowers synthesized by pulse electrodeposition. Fig. 2(A) shows the transmission electron microscopy (TEM) image of the nanopetals, which were mechanically scratched off the Pt nanoflower thin film. A selected-area electron diffraction (SAED) pattern is shown in the inset of the figure. The bright diffraction rings can be indexed as the (111), (200), (220) and (311) lattice planes of the Pt face-centered-cube (fcc) lattice structure. From the TEM image, the Pt nanopetals had a bamboo-leaf like structure, with an average length of

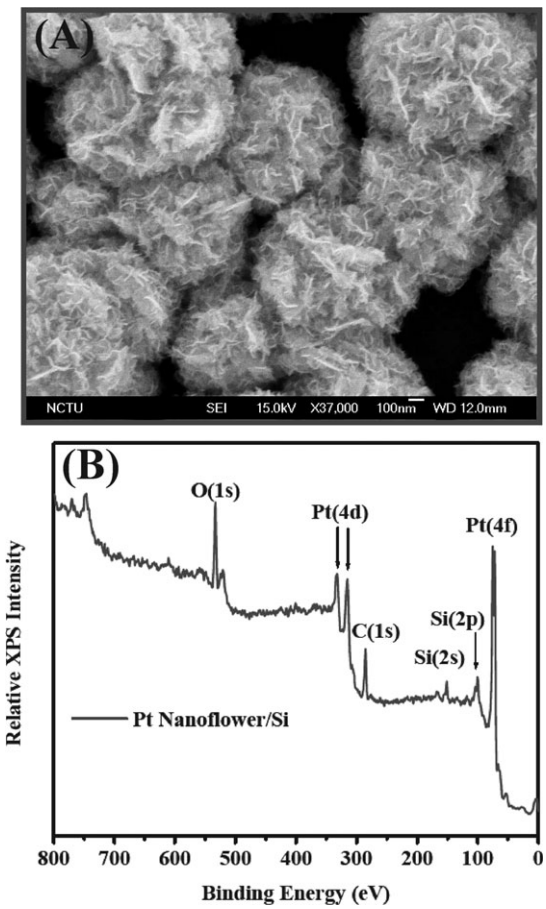

Fig. 1 (A) Scanning electron micrographs of the 3-D Pt nanoflower/Si surface and (B) XPS survey spectrum of the 3-D Pt nanoflowers on the silicon substrate.

[a] *Department of Materials Science and Engineering, National Chiao Tung University, 1001 Ta Hsueh Road, Hsinchu, 300, Taiwan R.O.C. E-mail: jnt_tiw123@yahoo.co.in, fmpan@faculty.nctu.edu.tw; Fax: +886 3-5724727; Tel: +886 3-5131322*
[b] *Department of Mechanical Engineering, National Taiwan University of Science & Technology, Taipei, 0660, Taiwan, R.O.C.*

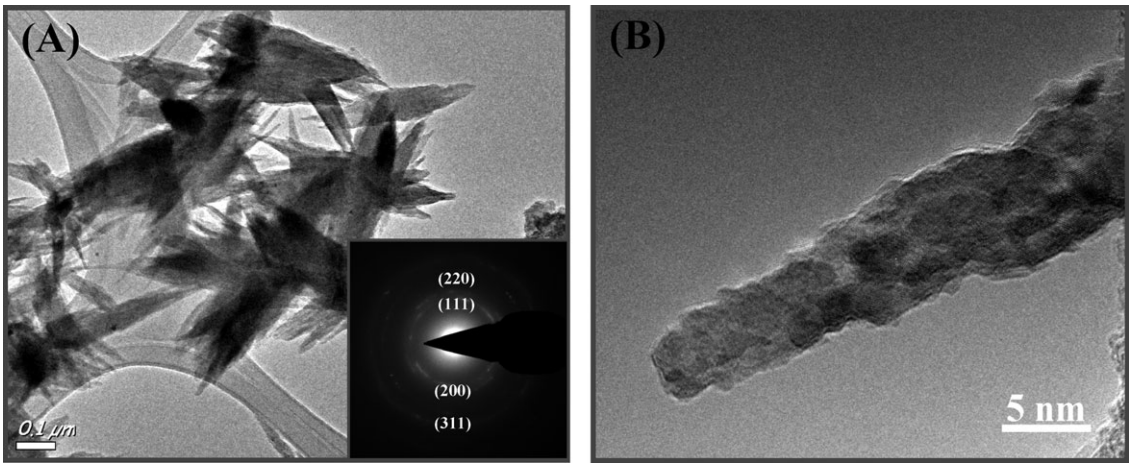

Fig. 2 (A) TEM of nanopetals mechanically scratched off the 3-D Pt nanoflower/Si sample. The inset shows the SAED pattern, and (B) a high resolution TEM image of a nanopetal.

~300 nm. The high resolution lattice image further reveals that the nanopetal was made up by Pt nanocrystals of a few nanometers in size as shown in Fig. 2(B).

The electroactive surface area of the catalyst was evaluated from charges associated with hydrogen adsorption/desorption on the electrode surface from cyclic voltammograms (CVs) in 1 M H_2SO_4 aqueous solution at a scan rate of 20 mV s^{-1}.[7] Fig. 3(A) shows CVs of the 3D Pt nanoflower/Si and the Pt thin film/Si electrodes. The Pt thin film/Si electrode was a blanket Pt thin film electrodeposited on the Si substrate for comparison. In the potential range characteristic of hydrogen electrosorption in sulfuric acid solution (−0.4 to 0.0 V *vs.* SCE), the Pt thin film/Si electrode shows a very weak and featureless broad peak, while two peaks (at *ca.* −0.22 and −0.02 V *vs.* SCE) can be clearly observed on the CV curve of the Pt nanoflower/Si electrode. The peak feature in a cyclic voltammogram of Pt in sulfuric acid solutions strongly depends on the crystallographic orientation of the Pt surface. For the Pt(111) surface, the cyclic voltammogram is characterized by a broad and flat hydrogen electrosorption peak in the potential range ~−0.4 to 0.0 V (*vs.* SCE).[8] On the other hand, in the same potential range, the Pt(100) surface gives two distinct hydrogen electrosorption peaks, and a single peak can be found for the Pt(110) surface in the same potential range. Thus, from the CV curves of Fig. 3(A), we suggest that the (100) and (110) lattice planes prevailed over the (111) plane on the 3D Pt nanoflower surface.

The hydrogen adsorption charge (Q_H) evaluated from Fig. 3(A) is ~0.27 and ~31.17 mC cm^{-2} for the Pt thin film/Si and the 3D Pt nanoflower/Si electrodes, respectively. Q_H is usually used to quantify active sites for hydrogen adsorption/desorption on the Pt catalyst. The measured Q_H values show that the active surface area of the 3D Pt nanoflowers/Si electrode is much higher than that of the Pt thin film/Si electrode by a factor of >110.

Electrocatalytic activity of the 3D Pt nanoflower/Si and the Pt thin film/Si electrodes toward methanol oxidation reaction (MOR) was studied by cyclic voltammetry in a nitrogen-saturated 1 M CH_3OH–1 M H_2SO_4 solution at a scan rate of 25 mV s^{-1}, and the CV curves are shown in Fig. 3(B). The onset potential for methanol oxidation of the 3D Pt nanoflower catalyst was ~0.38 V, which was ~0.13 V lower than that of the Pt thin film catalyst, indicating faster electrode kinetics.[9] In addition, the oxidation current peak density of the 3D Pt nanoflower catalyst in the forward scan was higher than that of the blanket Pt thin film catalyst. This implies that the 3D Pt nanoflower catalyst has a better electrocatalytic activity toward MOR compared with the blanket Pt thin film catalyst. In the CV scan, the anodic peak in the reverse scan might be attributed to the removal of CO-like poisoning species formed on the Pt catalyst in the forward scan. The catalyst tolerance against CO adsorption may be estimated by the ratio of the forward current density (I_f) to the reverse anodic peak current density (I_b), (I_f/I_b).[10] A high I_f/I_b ratio suggests efficient electrooxidation of methanol during the forward scan and less accumulation of residues on the electrodes, whereas a low ratio indicates incomplete electrooxidation of methanol and excessive accumulation of carbonaceous residues on the electrode surface. The (I_f/I_b) ratio of the 3D Pt nanoflower/Si electrode and the Pt thin film/Si electrode are ~2.5 and ~0.93, respectively. This ratio for the 3D Pt nanoflower/Si electrode is ~2.68 times larger than that for the Pt thin film/Si electrode, indicating that the 3D Pt nanoflowers electrode had a higher electrocatalytic activity toward MOR and thus a better CO tolerance.

To study CO tolerance of the 3D Pt nanoflower/Si electrode, CO-stripping CV measurement was carried out. Fig. 3(C) shows the CO stripping CV curves of the 3D Pt nanoflower/Si and the Pt thin film/Si electrodes in 1 M H_2SO_4 aqueous solution. For the CO stripping analysis, CO adsorption on the Pt catalyst was conducted by flowing a 10% CO–N_2 gas mixture into the (1 M H_2SO_4) electrolyte for 35 min at 0.1 V (*vs.* SCE), followed by purging with nitrogen gas for 30 min to remove any residual CO from the solution. As shown in Fig. 3(C), during the first cycle, the CV curve was flat in the potential range between −0.3 to 0.3 V indicating that the hydrogen adsorption was suppressed due to the complete coverage of available active Pt sites by CO adspecies. In the first scan, a broad anodic peak appeared between

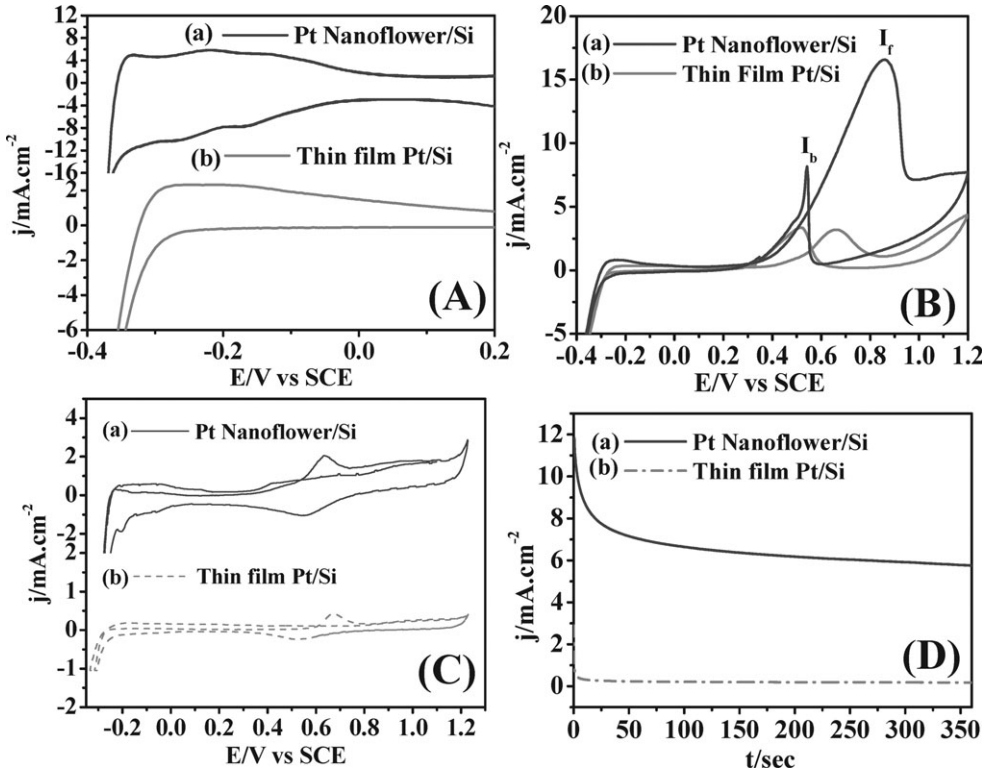

Fig. 3 Electrochemical measurements of the 3-D Pt nanoflower/Si and the Pt thin film/Si electrodes. (A) Cyclic voltammograms in 1 M H_2SO_4 solution at a scan rate of 20 mV s^{-1}; (B) Cyclic voltammograms in 1 M CH_3OH–1 M H_2SO_4 solution at a scan rate of 25 mV s^{-1}. (C) CO stripping cyclic voltammograms in CO saturated 1 M H_2SO_4 solution (the scan rate is 20 mV s^{-1} and CO adsorption occurs at +0.1 V *vs.* SCE). (D) Chronoamperograms in 1 M CH_3OH–1 M H_2SO_4 solution at a polarization potential of 0.4 V.

0.4 and 0.8 V, which was absent in the subsequent scan, indicating that CO adspecies were effectively oxidized during the first scan. The CO oxidation current peaks of the 3D Pt nanoflower/Si and the thin film Pt/Si electrodes were centered at ~0.58 and ~0.64 V, respectively. The peak current density of CO electrooxidation on the 3D Pt nanoflower/Si electrode was much larger than that on the Pt thin film electrode, further indicating that the 3D Pt nanoflower/Si electrode had a much larger electroactive surface area.

The above electrochemical analysis results indicate that the 3D Pt nanoflower/Si electrode possessed a much higher electrocatalytic activity towards CO oxidation and MOR compared to the Pt thin film/Si electrode. This may be ascribed to that Pt catalysts on the two electrodes had different preferential surface lattice orientations. It is known that methanol oxidation reaction catalyzed by Pt in acidic aqueous solutions is sensitive to the surface structure of the Pt catalyst.[11] According to previous reports, the electrocatalytic activity of Pt toward MOR in H_2SO_4 aqueous solution decreases in the order Pt(100) > Pt(110) > Pt(111).[12] As discussed above about the hydrogen eletrosorption peaks (Fig. 3(A)), the Pt nanoflower/Si electrode had more surface areas with the Pt(100) and Pt(110) lattice orientations than the blanket Pt thin film electrode, for which the catalyst surface was preferentially oriented as Pt(111). Therefore, as shown in Fig. 3(B), a lower onset potential and a much higher current density were obtained during the forward scan in the methanol oxidation CV measurement for the Pt nanoflower/Si electrode. In addition, the oxidation rate of CO adspecies on Pt also varies with the Pt surface orientation, with the electrocatalytic activity increasing in the order Pt(111) < Pt(110) < Pt(100).[13] As a result, CO-like adspecies on the Pt(100) and (110) surfaces can be oxidized more effectively than on the (111) surface, leaving more active sites for methanol adsorption. The better CO tolerance observed for the Pt nanoflower/Si electrode is likely also due to the preferential (100) and (111) surface orientation on the Pt catalyst.

Chronoamperometry was used to compare the stability of the electrocatalytic activity toward MOR of the 3D Pt nanoflower/Si electrode with that of the Pt thin film/Si electrode. Fig. 3(D) shows the chronoamperograms of the two electrodes, which were obtained by measuring the steady-state reaction current density at the electrode potential of 0.4 V. After polarization for 350 s, the current densities of methanol electrooxidation for the Pt thin film/Si and the 3D Pt nanoflower/Si electrode were ~0.02 and ~6.2 mA cm^{-2}, respectively. Compared with the blanket Pt thin film, the 3D Pt nanoflower/Si had a much higher activity with a steady-state current density about 310 times that of the thin film Pt/Si electrode. These results are fully consistent with the CV measurements shown in Fig. 3(A)–(C).

Electrochemical impedance spectroscopy (EIS) is a powerful analysis technique, which can provide a wealth of information on the charge transfer resistance and capacitance. The Nyquist plots of the 3D Pt nanoflower/Si and the Pt thin film/Si electrodes at the potential of 0.3 V in 1 M CH_3OH–1 M

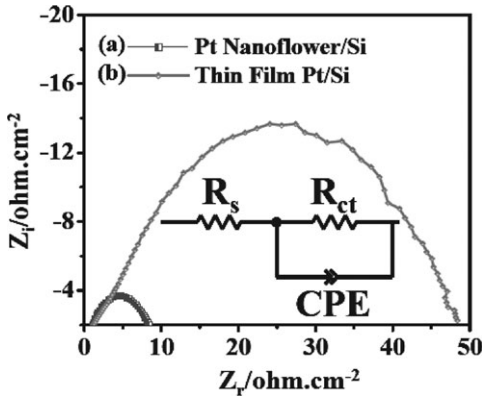

Fig. 4 Nyquist plot of electrochemical impedance spectra (EIS) of the 3D Pt nanoflowers and the Pt thin film catalysts in 1 M CH_3OH–1 M H_2SO_4 solution at the potential of 0.3 V. The inset shows the equivalent circuit model used to fit the impedance spectra.

H_2SO_4 aqueous solution are shown in Fig. 4, where Z_r and Z_i are the real and imaginary parts of the impedance. The thin lines are fitting results according to the equivalent circuit shown as the inset in Fig. 4; R_s denotes the solution resistance, R_{ct} represents the charge-transfer resistance and CPE is defined as the constant phase element, which takes into account methanol adsorption and oxidation.[14] As shown in Fig. 4, the proposed model fits well to the obtained EIS data points. The charge-transfer resistances at the 3D Pt nanoflower/Si and the Pt thin film/Si electrodes were $\sim$9 and $\sim$50 Ω cm^{-2}, respectively. The very low R_{ct} obtained with the Pt nanoflower/Si electrode suggests that this type of electrode could be suitable for direct methanol fuel cell applications.

In summary, we have demonstrated a facile and reproducible method to synthesize 3D Pt nanostructures on silicon substrates at room temperature by potentiostatic pulse plating. The Pt nanostructure is made up of bamboo-leaf-like nanopetals, and has an overall rose-like structure. Electrochemical analysis show that the 3D Pt nanoflowers had a much larger active surface area than the Pt thin film by a factor of $>$110, and were likely preferentially oriented in the (100) and (110) surface planes. Due to the preferential surface orientations and high surface area, the 3D Pt nanoflower catalyst had an excellent electrocatalytic activity toward methanol oxidation and a high CO tolerance as compared with the Pt thin film catalyst.

Experimental

A p-type 4-inch Si wafer of low resistivity (0.002 Ω-cm) was used as the substrate for the synthesis of the 3D Pt nanoflowers. 1 M H_2PtCl_6 (Sigma-Aldrich) was first mixed with 1 M H_2SO_4 (Sigma-Aldrich) in an aqueous solution at room temperature, and the mixture was stirred at 25 °C for 5 h to make the mixture solution homogeneous. The Pt catalyst was then electrodeposited on the flat silicon substrate in the mixed solution by potentiostatic pulse plating in a three-electrode cell system with a saturated calomel reference electrode (SCE). The time periods for the positive potential pulse (+0.05 V) and the negative potential pulse (−0.02 V) were 5 and 1 ms, respectively. Under the bipolar pulse electrodeposition conditions, 3D Pt nanoflowers could be synthesized on the Si substrate. After Pt electrodeposition, the sample was washed with DI water to remove contamination from the sample surface, and dried under ambient conditions.

Electrochemical experiments were carried out using an electrochemical workstation (Jihan 5000). All the electrochemical experiments were performed in a three-electrode system. The saturated calomel electrode (SCE), a Pt wire and the Pt catalyst were used as the reference, counter and working electrode, respectively. Cyclic voltammograms were obtained in N_2 saturated 1 M H_2SO_4 and 1 M CH_3OH–1 M H_2SO_4 aqueous solutions at room temperature. All the aqueous solutions were prepared using low resistance ($\sim$18 MΩ) DI water produced by a Milli-Q water purification system.

Surface morphology was examined by a JEOL JSM-6700F scanning electron microscope. TEM micrographs were obtained by a JEOL JEM-3000F transmission electron microscope operated at 200 kV. The TEM specimen was prepared by mechanically scratching the nanoflower thin film using dissecting forceps in the presence of a small drop of ethanol. The scratched specimen was put onto a holey-copper grid and dried in air at room temperature. X-Ray photoelectron spectroscopy (XPS, Thermo VG 350) was used to study the surface chemical composition of the nanoflowers using Mg-Kα radiation (1253.6 eV).

Acknowledgements

This work was supported by the National Science Council of R.O.C., under Contract No. NSC93-2120-M-009-007. Technical support from the National Nano Device Laboratories (NDL) is gratefully acknowledged.

References

1 (*a*) X. Teng, X. Liang, S. Rahman and H. Yang, *Adv. Mater.*, 2005, **17**, 2237; (*b*) J. N. Tiwari, T. M. Chen, F. M. Pan and K. L. Lin, *J. Power Sources*, 2008, **182**, 510; (*c*) J. N. Tiwari, F. M. Pan, R. N. Tiwari and S. K. Nandi, *Chem. Commun.*, 2008, (48), 6516.
2 X. Peng and A. Chen, *Adv. Funct. Mater.*, 2006, **16**, 1355.
3 S. Hrapovic, Y. L. Liu, K. B. Male and J. H. T. Luong, *Anal. Chem.*, 2004, **76**, 1083.
4 (*a*) R. F. Service, *Science*, 1999, **285**, 682; (*b*) K. V. Kordesch and G. R. Simader, *Chem. Rev.*, 1995, **95**, 191.
5 A. Rouxoux, J. Schulz and H. Patin, *Chem. Rev.*, 2002, **102**, 3757.
6 P. Marcus and C. Hinnen, *Surf. Sci.*, 1997, **392**, 134.
7 D. Kardash and C. Korzeniewski, *Langmuir*, 2000, **16**, 8419.
8 M. Bergelin, J. M. Feliu and M. Wasberg, *Electrochim. Acta*, 1998, **44**, 1069.
9 A. V. Tripkovic, S. Strbac and K. Dj. Popovic, *Electrochem. Commun.*, 2003, **5**, 484.
10 Z. L. Liu, X. Y. Ling, X. D. Su and J. Y. Lee, *J. Phys. Chem. B*, 2004, **108**, 8234.
11 Y. G. Liu, S. L. Shi, X. Y. Xue, J. Y. Zhang, Y. G. Wang and T. H. Wang, *Appl. Phys. Lett.*, 2008, **92**, 203105.
12 T. H. M. Housmans, A. H. Wonders and M. T. M. Koper, *J. Phys. Chem. B*, 2006, **110**, 10021.
13 N. M. Markovic and P. N. Ross, Jr, *Surf. Sci. Rep.*, 2002, **45**, 117.
14 K. Koczkur, Q. Yi and A. Chen, *Adv. Mater.*, 2007, **19**, 2648.